

Many-body study of a quantum point contact in the fractional quantum Hall regime at $\nu = 5/2$

Paul Soulé¹, Thierry Jolicoeur¹, and Philippe Lecheminant²

¹*Laboratoire de Physique Théorique et Modèles statistiques, Université Paris-Sud, 91405 Orsay, France and*

²*Laboratoire de Physique Théorique et Modélisation,
CNRS UMR 8089, Université de Cergy-Pontoise, Site de Saint-Martin,
2 avenue Adolphe Chauvin, 95302 Cergy-Pontoise Cedex, France*

(Dated: July 14th, 2013)

We study a quantum point contact in the fractional quantum Hall regime at Landau level filling factors $\nu = 1/3$ and $\nu = 5/2$. By using exact diagonalizations in the cylinder geometry we identify the edge modes in the presence of a parabolic confining potential. By changing the sign of the potential we can access both the tunneling through the bulk of the fluid and the tunneling between spatially separated droplets. This geometry is realized in the quantum point contact geometry for two-dimensional electron gases. In the case of the model Moore-Read Pfaffian state at filling factor $\nu = 5/2$ we identify the conformal towers of many-body eigenstates including the non-Abelian sector. By a Monte-Carlo technique we compute the various scaling exponents that characterize the edge modes. In the case of hard-core interactions whose ground states are exact model wavefunction we find equality of neutral and charged velocities for the Pfaffian state both bosonic and fermionic.

I. INTRODUCTION

Modern semiconductor technology has made it possible to fabricate structures with electronic motion essentially restricted to two dimensions¹. In these so-called two-dimensional electron gases (2DEG) the motion along the direction perpendicular to the sample plane is frozen into its quantum-mechanical ground state. This may be realized in heterostructures and in quantum wells. They differ in the shape of the wavefunction for the frozen motion. The mesoscopic physics at play in 2DEGs is very rich and includes the integer and fractional quantum Hall effects, quantum localization and double-barrier tunneling. One of the main building blocks of mesoscopic devices is the so-called “quantum point contact” (QPC) : a constriction of the 2D electronic fluid created by the electrostatic potential of a gate. Tuning the potential allows to control the shape of the electron droplet. Devices like interferometers involve typically several QPCs. When used in the quantum Hall regime they allow manipulation of the edge modes that propagate at the boundary of the sample. It is possible to increase the tunneling rate between edges by inducing a pinching of the 2DEG. By measuring the noise characteristics of this geometry it has been shown^{2,3} that quasiparticles at filling factor $1/3$ in the fractional quantum Hall (FQH) regime have fractional charge $1/3$ as expected from Laughlin’s theory⁴.

The simplest description of these phenomena is by an effective theory that keeps only the low-energy edge modes that are generically present in FQH liquids⁵⁻⁸. In this framework the simplest FQH fluids at filling factor $\nu = 1/m$ have low-energy excitations described by a free chiral boson theory at each edge. Complicated samples with multiply-connected geometry involve in general several such modes even if the electron fluid stays at $\nu = 1/m$. When the filling factor is not simple, for example in the Jain sequence $\nu = p/(2p + 1)$, edge states are described by several interacting chiral bosons. Detailed understanding of these modes is still controversial⁹⁻¹⁸. Even more intriguing is the case of the fraction $\nu = 5/2$ which is believed to be described by the Moore-Read¹⁹ Pfaffian state (or its particle-hole conjugate dubbed the antipfaffian). This elusive FQH state has a fermionic Majorana edge mode in addition to a chiral bosonic mode and interferometers have been proposed to manipulate the associated quasiparticles and reveal their non-Abelian statistics²⁰. Typical devices like Fabry-Perot interferometers involve several QPCs. As a function of the gate voltage there are typically two limiting regimes. When the voltage is small the pinching of the 2DEG leads to a smaller distance between edges and hence tunneling of quasiparticles is possible through traversal of the bulk liquid. When the voltage is very large one may reach the so-called pinch-off regime where the droplet is now cut into two separate islands and only electron tunneling between them is allowed. The theoretical treatment of these two situations can be done by adding ad-hoc operators to the effective bosonic field theory, encapsulating all microscopic tunneling details into a few coupling constants. The quasiparticle creation operator has then to be expressed in terms of the effective Bose degrees of freedom, as is the case for the electron operator. Many experimental features can be explained in this framework¹³. Nevertheless it is important to have a microscopic understanding of the phenomena. Previous numerical studies of microscopic models have used the disk geometry²¹⁻²⁶ to evaluate tunneling matrix elements for the fillings $\nu = 1/3$ as well as $\nu = 5/2$. It is also possible up to some extent to identify the edge mode quantum numbers and measure velocities.

In this paper we study the FQH effect in a QPC by using the cylinder geometry²⁷⁻²⁹. In the Landau gauge one can

impose periodic boundary conditions along one direction and keep the other one free. It is then possible to perform exact diagonalization (ED) studies of various Hamiltonians for small numbers of particles. This gauge also allows the addition of a parabolic confining potential to lift the edge mode degeneracy. We first use a hard-core interaction two-body interaction to create a $\nu = 1/3$ FQH droplet. The spectrum of low-lying modes can be analyzed in terms of a Luttinger model³⁰. While this is known for the case of a positive potential²⁸ we show that if the harmonic potential is reversed (with hard walls to keep it bounded from below) then the fluid separates in two droplets and that the two disconnected edges again combine in a non-chiral Luttinger liquid. The study of the spectrum allows us to identify the zero modes of the effective bosonic theory and their role in the description of electron tunneling. Measurement of the Luttinger exponent reveals the duality between quasiparticle and electron properties as expected from theory^{31–35}.

We also study the Moore-Read Pfaffian state in the QPC geometry by using the special three-body hard-core Hamiltonian whose ground state is the Pfaffian. The mode counting reflects the fractionalization of the charge in units of $e/4$. In the spectrum we are able to identify the various bosonic and fermionic excitations that form conformal towers as expected from conformal field theory (CFT). While there is a set of low-energy states that corresponds to almost rigid translation of the incompressible droplet this is not the only possibility and we also find a series of states that are generated by transfer of a $e/4$ quasiparticle through the droplet. The associated conformal towers now are described in terms of the spin scaling field in the Ising CFT. It is an important feature of the cylinder geometry that the non-Abelian sector appears in a natural way as a function of the total momentum of the ground state and does not require tweaking extra potentials to locate a quasiparticle at the origin of a disk or at the pole of a sphere. The low-lying energies of the CFT towers can be analyzed to find the charge Luttinger parameter as in the plain Laughlin liquid case but lead also to the measurement of the non-trivial scaling dimensions of the Ising fields. While ED studies are limited to numbers of particles too small to extract the scaling dimensions, we introduce a Monte-Carlo method based on the exact formulas for Pfaffian edge states in all sectors to compute reliably the scaling dimension of spin field σ as well as of the Majorana field θ . The bosonic Pfaffian at $\nu = 1$ share the same spectral features. For the special hard-core Hamiltonians that generate exactly the wavefunctions we find unexpectedly that the Bose and Fermi velocities are equal or almost equal in the thermodynamic limit which implies that the special interactions have an extended symmetry.

In section II, we present the cylinder geometry and discuss the introduction of a parabolic potential. In section III, we add a parabolic potential well to lift the degeneracy of the edge states and compute the Luttinger parameter g in the simple case of a principal Laughlin $\nu = 1/m$ in the two possible geometries of the QPC, the weak constriction regime and the pinch-off regime. In section IV we explain the basics of the Moore-Read Pfaffian edge modes in the disk geometry. Then we explore the conformal towers in the cylinder geometry in section V. Finally we present a Monte-Carlo method to obtain accurate measurements of scaling dimensions in section VI. Our conclusions are presented in section VII.

II. THE QPC IN THE CYLINDER GEOMETRY

To study FQH physics on the cylinder one has first to use the Landau gauge which is compatible with periodic boundary conditions in one space direction. We take the vector potential as $A_x = 0$ and $A_y = Bx$ and the one-body eigenstates in the lowest Landau level (LLL) are given by :

$$\phi_n(x, y) = \frac{1}{\sqrt{L\sqrt{\pi}}} e^{-\frac{1}{2}(x-k)^2} e^{iky} = \frac{1}{\sqrt{L\sqrt{\pi}}} e^{-\frac{2\pi^2}{L^2}n^2} Z^n e^{-x^2/2}, \quad Z \equiv e^{\frac{2\pi}{L}(x+iy)}. \quad (1)$$

Here we have set the magnetic length $\ell = \sqrt{\hbar c/eB}$ to unity. The periodic direction y has a length L and the momentum k is quantized $k = 2\pi n/L$ with n an integer (which can be negative or positive). All the states ϕ_n are degenerate and constitute the basis on which we construct the Fock space. If we add a potential energy $V(x)$ invariant by translation along the cylinder periodic direction y then it appears in the Hamiltonian through its matrix element :

$$\tilde{V}_n = \frac{1}{L\sqrt{\pi}} \int dx e^{-(x - 2\pi n/L)^2} V(x). \quad (2)$$

To deal with a finite-dimensional Fock space we impose a cut-off on the values of the integer n . This procedure allows ED of the Hamiltonian by linear algebra techniques standard in the field of strongly correlated systems. This type of cut-off physically resembles a cut-off in real space only in the limit when the length $L \rightarrow 0$. Here the orbitals are widely separated by more than the magnetic length and any reasonable confining potential gives rise to such a boundary condition. In the opposite limit $L \rightarrow \infty$ there is *no* non-oscillating potential leading to a hard cut-off in reciprocal space. This leads ultimately to the appearance of spurious low-energy modes that do not belong to the true FQHE problem²⁸. However if we keep an aspect ratio reasonably close to unity, then the physics of the FQHE

is present in this geometry. The limit $L \rightarrow 0$ is known as the Tao-Thouless limit (TT)^{36–41}. The problem becomes closer to an electrostatic problem and many features of the FQHE can be analyzed simply. However in the TT limit the ground state becomes a Slater determinant with a trivial entanglement spectrum. Nevertheless the fusion rules for quasiparticles still remain complete⁴². We show in this paper that this is also an appropriate limit to identify the so-called conformal towers of excited states.

Generically the two-body interaction projected in the LLL can be written as a function of projection operators of the state of relative angular momentum m for each pair of particle :

$$\mathcal{H}_{int} = \sum_{i < j} \sum_m V_m \hat{P}_{ij}^{(m)}, \quad (3)$$

where the coefficients V_m are the so-called³⁰ Haldane pseudopotentials. While originally defined in the disk geometry they can be extended to the cylinder case as shown by Rezayi and Haldane⁴³. Spinless fermions are only sensitive to odd values of m and of particular interest is the extreme hard-core model for which the only nonzero pseudopotential is V_1 . In this peculiar case the Laughlin wavefunction is the exact unique zero-energy ground state. A fictitious potential reproducing an arbitrary set of V_m s is given by $\tilde{V}(q) = \sum V_m L_m(q^2)$ where the L_m s are the Laguerre orthogonal polynomials. It can be then inserted in the second-quantized expression of the Hamiltonian :

$$\mathcal{H}_{int} = \frac{1}{2} \sum_{\{m_i\}} \mathcal{A}_{m_1, m_2, m_3, m_4} c_{m_1}^\dagger c_{m_2}^\dagger c_{m_3} c_{m_4}, \quad (4)$$

with the matrix elements given by :

$$\mathcal{A}_{m_1, m_2, m_3, m_4} = \frac{1}{2L} \int \frac{dq}{2\pi} \tilde{V}(q, \frac{2\pi}{L}(m_1 - m_4)) e^{-q^2/2 + 2i\pi q(m_1 - m_3)/L} e^{-2\pi^2(m_1 - m_4)^2/L^2}, \quad (5)$$

where $\tilde{V}(q_x, q_y)$ is the ordinary Fourier transform of the potential. In the present work we use a potential that produces only V_1 and V_3 given by :

$$\tilde{V}(q_x, q_y) \equiv \tilde{V}(\mathbf{q}) = -(V_1 + 3V_3)\mathbf{q}^2 + \frac{3}{2}V_3\mathbf{q}^4 - \frac{1}{6}V_3\mathbf{q}^6, \quad (6)$$

where we set $\mathbf{q}^2 = q_x^2 + q_y^2$. The coefficients for the third pseudopotential can be checked by verification that the Hamiltonian has a unique zero-energy ground state for filling factor $\nu = 1/5$ obtained by imposing the (Laughlin) relation between the number of orbitals and the number of electrons.

If we want to study the Pfaffian state then one needs to consider a special three-body Hamiltonian with derivative interactions whose exact zero-energy ground-state is given by the Pfaffian wavefunction introduced by Moore and Read¹⁹ :

$$\mathcal{H}_3 = - \sum_{i < j < k} \mathcal{S}_{ijk} \Delta_i^2 \Delta_j \delta^2(\mathbf{r}_i - \mathbf{r}_j) \delta^2(\mathbf{r}_j - \mathbf{r}_k), \quad (7)$$

where \mathcal{S} stands for symmetrization. To perform ED studies the Fock space should be finite-dimensional. This is enforced by restricting the allowed orbitals to a finite range of momenta : the integer n indexing the one-body wave functions takes only $2K_{max} + 1$ values. This allowed range can be translated at will as long as there is complete translation invariance along the cylinder. For example if we take $0 \leq n \leq 2K_{max}$ then the Z powers are positive and formal expressions of first-quantized wavefunctions are closest to the disk geometry. Centering the range of n values at zero momentum is more natural if we add a parabolic potential to mimic a realistic QPC geometry. To create a droplet of Laughlin-type fluid at filling $1/3$ one chooses $2K_{max} = 3(N - 1)$ while the Pfaffian requires the adjustment $2K_{max} = 2N - 3$ exactly as in the spherical geometry. Adding orbitals beyond this reference number leads to the appearance of more zero-energy states that are the gapless edge states of the FQHE fluid. In the cylinder geometry there are *two* counterpropagating edges that combine into non-chiral effective theories. To reveal their precise content it is convenient both physically and practically to add an extra parabolic potential well along the axis of the cylinder which is invariant under y translations so that the total momentum remains a good quantum number : $V = \beta \sum_k k^2 n_k$. We define the conserved total momentum as K_{tot} whose values are integers or half-integers that can be used to label the many-body eigenstates (this momentum is thus in units of $2\pi/L$).

If the coefficient β is taken to be positive then a quantum Hall droplet will stay centered in the middle of the cylinder and, provided we allow enough extra orbitals, there will be two edges that can combine. This is displayed in Fig.(1) and Fig.(2). If we now use a negative β value leading to a inverted potential then the droplet splits into two separate chunks each of them using the more energetically favorable orbitals closest to the hard wall in k -space,

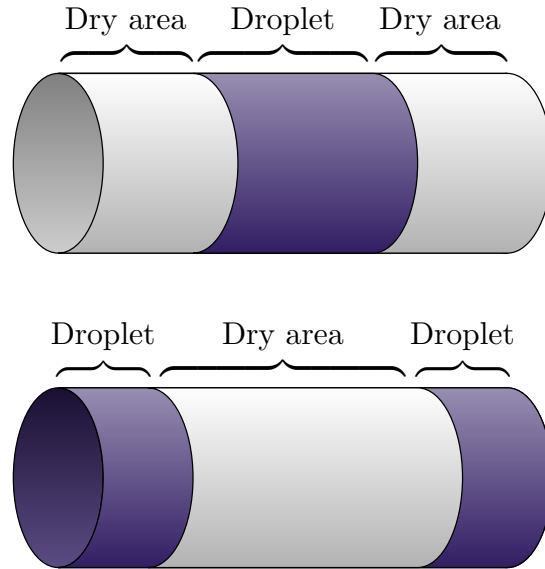


FIG. 1: The location of the quantum Hall droplet according to the value of the potential along the axis of the cylinder. Top panel : the potential is convex leading to a single droplet (blue area) centered in the middle of the cylinder. Bottom panel : with a concave potential it is more favorable to split the liquid into two occupied areas close to the hard walls. The edge modes then reside at the boundary between the droplet(s) and the dry area(s).

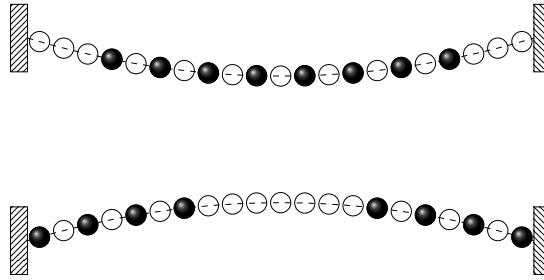


FIG. 2: The root configuration of a bosonic Laughlin state at $\nu = 1/2$ in the two possible configurations mimicking the QPC geometry. Top view shows the middle droplet while the bottom view shows the configuration with two spatially separated droplets.

provided that the potential well is deep enough. In the following studies we use a potential small enough so that there is always a large separation between bulk and edge states : see Fig.(3) for a typical situation.

Since we use a parabolic external potential $V = \beta \sum_k (k - k_0)^2 n_k$, it satisfies :

$$[V, U] = \beta U^p \sum_k \{(k - k_0 + p)^2 - (k - k_0)^2\} n_k = \beta U^p (2pK + p^2N), \quad (8)$$

where $U \propto \prod_i Z^i$ is the translation operator of one orbital along the x axis, and $K = \sum_k (k - k_0) n_k$ the momentum operator with the convention that the ground state wavefunction has zero momentum. Therefore, if $|\psi\rangle$ is an eigenstate of our total Hamiltonian $\mathcal{H}_{int} + V$ with energy E , N particles and momentum K , then $U^p |\psi\rangle$ is also an eigenstate with energy and momentum :

$$E' = \beta(2pK + p^2N), \quad K' = K + pN. \quad (9)$$

So, provided there are no hard walls or if the walls are far enough (large K_{max}), it is possible to deduce the whole spectrum from the sector with $K = 0, \dots, N - 1$. It can be used in an approximate way if we add enough orbitals beyond that required by the flux-number of electrons that defines our FQH state.

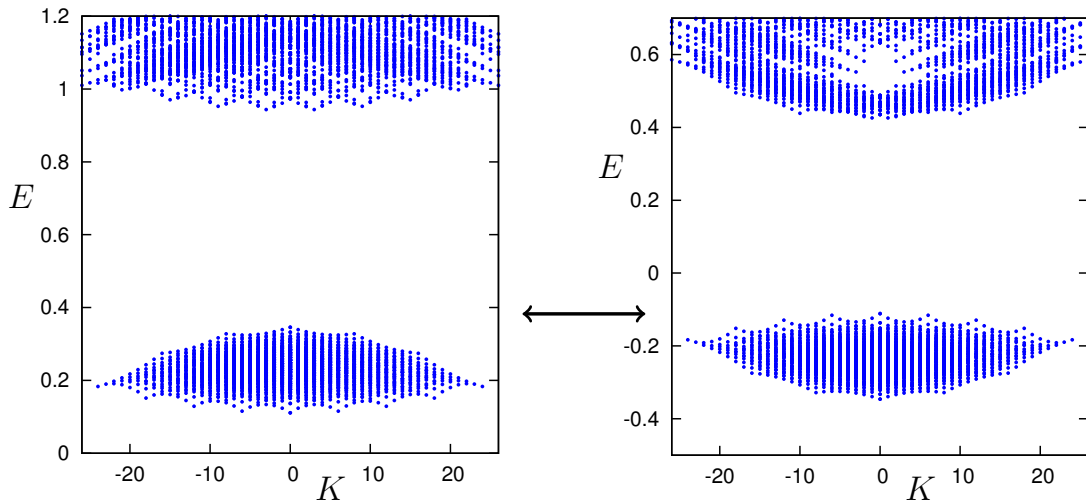


FIG. 3: The two QPC configurations in the limit of a small parabolic potential. Here we plot the spectrum of $N = 6$ electrons in orbitals describing the $\nu = 1/3$ Laughlin state and edge excitations. Left panel: single droplet regime where the cusps in the low-lying states are related to quasiparticle transfers. Right panel: we change the sign of the confining potential to switch to the pinch-off regime. Now the cusps are due to electron tunneling. Since the potential is taken to be weak, first-order perturbation theory means that one just reverse the manifold of edge states.

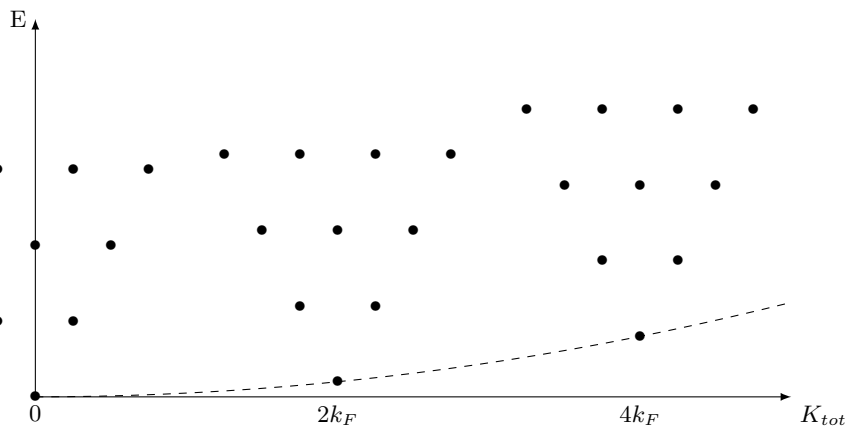


FIG. 4: The spectrum of a free non-chiral boson theory with finite radius. There are sectors at $K = 0, 2k_F, 4k_F, \dots$ that are similar to the spectrum of a non-compact boson. The extra excitations associated with non-trivial windings leads to copies of the $k = 0$ spectrum shifted quadratically in energy. The finite-size spectrum of free fermions is the same. The Luttinger parameter value is encoded in the parabolic shift of the energy. The special spectra above each extremal point at $2nk_F$ are the so-called conformal towers of the bosonic CFT.

III. LUTTINGER LIQUID AND THE ABELIAN QPC

The Lagrangian of the chiral Luttinger model describing edge excitations of a Hall sample with two counterpropagating edges around an incompressible FQH liquid at filling $\nu = 1/m$ is given by^{8,13}:

$$\mathcal{L} = \mathcal{L}_R + \mathcal{L}_L = \frac{1}{4\pi g} \{ \partial_x \phi_R (i\partial_\tau + v\partial_x) \phi_R + \partial_x \phi_L (-i\partial_\tau + v\partial_x) \phi_L \}, \quad (10)$$

where the Luttinger parameter g is equal to the filling factor $g = \nu$. This effective theory does not include edge interactions and is presumably valid when there is a large spatial separation between them. The Hamiltonian that follows can be written as :

$$\mathcal{H} = \frac{v}{4\pi g} \int_0^L dx \{ (\partial_x \phi_L)^2 + (\partial_x \phi_R)^2 \}. \quad (11)$$

To expand this Hamiltonian into Fourier modes, one has to keep track of the zero modes that comes from the periodicity of the bosonic fields :

$$\mathcal{H} = \frac{\pi v}{gL}(N_L^2 + N_R^2) + \sum_{q \neq 0} v|q|b_q^\dagger b_q, \quad (12)$$

where b_q^\dagger, b_q are the Fourier mode creation/annihilation operators and $N_{L,R}$ are the winding numbers of the bosonic fields along the edge :

$$\phi_{L,R}(x+L) - \phi_{L,R}(x) = 2\pi N_{L,R}. \quad (13)$$

Quasiparticle states corresponds to fractional values of these parameters $N = n\nu$ with n integer while electron states are generated with $N = n$. This can be seen by computing the electric charge associated with the winding through $\rho = \partial_x \phi / 2\pi$. The momentum operator of this theory has a zero mode contribution in addition to the phononlike part :

$$K = k_F J + \sum_{q \neq 0} qb_q^\dagger b_q, \quad (14)$$

where the even integer J counts essentially the particle-hole excitations across the pseudo-Fermi surface with Fermi momentum k_F . Finally we note that the number of states at a given energy for a given chirality is determined by the partitions of unity and this can be obtained easily by expanding the character :

$$\chi_B(q) = \prod_{n=1}^{\infty} \frac{1}{(1-q^n)}. \quad (15)$$

This character is that of a free boson CFT. The level scheme we expect from the Luttinger picture is shown in Fig.(4).

If we now compute by exact diagonalization the spectrum of an electron system with a small quadratic potential then we find a characteristic Luttinger-like spectrum with arches interpolating between quasi-ground states separated by momenta $K = \pm N_e, \pm 2N_e, \pm 3N_e, \dots$. By adiabatically following these quasi-ground states when sending the potential to zero, we can identify their root configuration. In fact they are obtained by a global uniform translation of the Laughlin state from Eqs.(8,9). For neighboring quasi-ground states the shift is by exactly one orbital. This operation can be realized by threading the cylinder with a thin solenoid and increasing adiabatically the flux by one quantum. This is the celebrated Laughlin argument for quasiparticle creation. Electron are then pushed along the axis of the cylinder by exactly one orbital at the end the process. This is equivalent to the transfer of a fractionally charged quasiparticle from one edge of the system to the other edge. These quasiparticle transfers generate the whole set of extremal states that are prominent in Fig.(3). On top of these global excitations we can of course excite phononlike density modes with two possible chiralities corresponding to the two edges of the quantum Hall droplet. These excitations are created by acting with the b_q^\dagger Fourier mode operators. We identify the modes that are above each of the extremal states as phonon modes. The counting we find in ED studies is always compatible with the bosonic counting rule Eq.(15). From Eq.(12) we see that extracting the energies of the parabola of extremal states lead to an estimate of the Luttinger parameter, provided we have an independent measurement of the velocity v of phonon excitations. This strategy was already applied in the weak constriction regime²⁸. Here we note that it may also be applied in the complementary case of the QPC in the pinch-off regime where the fluid is now separated into two droplets. Indeed the global contribution to the Hamiltonian Eq.(11) can be written as :

$$\mathcal{H}_{global} = \frac{\pi v}{2\nu L}(J^2 + N^2), \quad (16)$$

where $J = N_L - N_R$ ($N = N_L + N_R$) is an integer that changes by two units for each transfer of an electron from the left droplet to the right droplet. This integer J indexes the extremal low-lying states of the Luttinger spectrum in Fig.(3) in the split QPC regime. Fitting the global parabolic envelope of the spectrum in this regime leads then to the *dual* exponent $g = 1/\nu = 3$ as expected from the standard duality⁸ between electrons and quasiparticles. Even with small system sizes we obtain a precise estimate of g : see Fig.(5).

We finally note that the tower structure of the principal Laughlin fluid can also be revealed by computing the entanglement spectrum⁴⁴⁻⁴⁶. However this approach does not lead to estimates of the boson radius.

IV. THE PFAFFIAN EDGE STATES IN THE DISK GEOMETRY

We now turn to the study of the model wavefunction known as the Moore-Read Pfaffian¹⁹. We first recall for completeness the knowledge about edge modes in the disk geometry before turning to the analysis in the cylinder

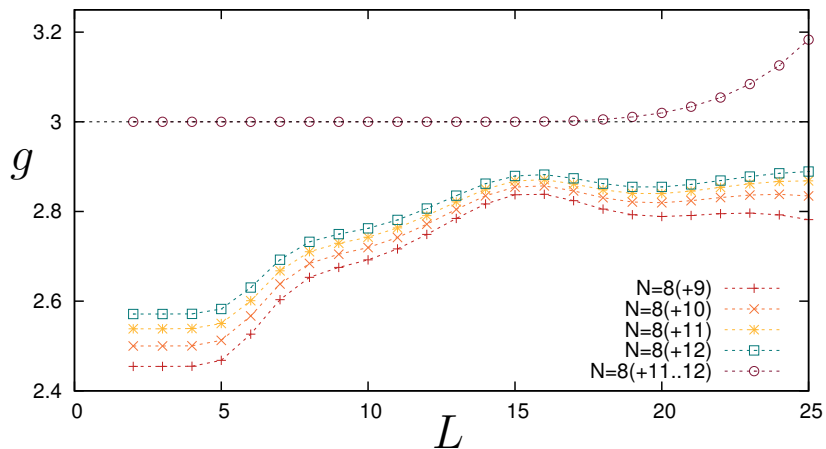


FIG. 5: Numerical estimation of the Luttinger parameter in the electron-tunneling configuration for two $\nu = 1/3$ spatially separated FQH droplet. The first four curves at the bottom are obtained from the edge spectrum for $N = 8$ with fixed number of extra orbitals. The topmost curve, circle markers, is an estimation using the finite size scaling explained in section VI with 11 and 12 extra orbitals. We also find that adding a small V_3 pseudopotential does not change the value of the exponent.

geometry with confining potential modeling a constriction in the $\nu = 5/2$ state. The formula for the Pfaffian state in the disk geometry is :

$$\Psi_{MR}(z_i) = \text{Pf}\left(\frac{1}{z_i - z_j}\right) \prod_{i < j} (z_i - z_j)^m, \quad (17)$$

where the symbol Pf stands for the Pfaffian of a matrix :

$$\text{Pf}(A_{ij}) = \sum_{\sigma} \epsilon_{\sigma} A_{\sigma(1)\sigma(2)} \cdots A_{\sigma(N-1)\sigma(N)}, \quad (18)$$

where ϵ_{σ} is the signature of the permutation σ . The corresponding filling factors are $\nu = 1$ in the Bose case and $\nu = 1/2$ in the Fermi case. In some 2DEGs with very high mobility there is an incompressible state in the second LL with total filling $5/2 = 2 + 1/2$ which is a strong candidate to be described by this wavefunction²⁰. Bosons with low-energy scattering in the s-wave are also an interesting candidate for the $m = 1$ state above^{47,48}. This model wavefunction can be generated as the zero-energy eigenstate of the three-body hard-core Hamiltonian Eq.(7). The edge modes of these fractions have been studied by Wen⁴⁹ and Milovanovic and Read⁵⁰. They include the charged modes that we have already discussed in the case of the elementary Laughlin fractions at filling $\nu = 1/m$. They are generated by multiplying the wavefunctions by a symmetric polynomial. The counting is given by a free bosonic mode Eq.(15). However this is not the whole story : there are also extra neutral modes that can be described by a Majorana fermion theory. From the point of view of the wavefunction, they are generated by removing some of the $1/z$ pairing-type factors and replacing them by powers of the coordinates :

$$\Psi_{n_i} = \mathcal{A}(z_1^{n_1} z_2^{n_2} \cdots z_F^{n_F} \frac{1}{z_{F+1} - z_{F+2}} \cdots \frac{1}{z_{N-1} - z_N}) \prod_{i < j} (z_i - z_j)^m, \quad (19)$$

where \mathcal{A} means antisymmetrization. The non-negative and distinct integers $0 \leq n_1 < \cdots < n_F$ can be interpreted as the occupation numbers of a fermion. Note that in this formula the number of electrons N can be odd or even (contrary to our basic Pfaffian definition Eq.(17)) but the difference $N - F$ should be even. This set of states can be counted by a Majorana-Weyl field theory provided we use antiperiodic boundary conditions on the field operator θ . This field theory can be written in a Lagrangian language :

$$\mathcal{L}_M = i\theta(\partial_t - v_n \partial_x)\theta, \quad (20)$$

where v_n is the velocity of the fermionic modes. It is nonzero only in the presence of an external potential such as the one created in a QPC. The antiperiodic sector $\theta(x+L) = -\theta(x)$ is called the Neveu-Schwarz (NS) sector. These edge modes are essentially unaffected by the presence of Abelian (i.e. Laughlin) quasihole in the bulk liquid, here in the interior region of the circular droplet. However the Pfaffian state of matter also include quasiholes with $e/4$ electric

I	1 0 1 1 2 2 3 3 5	NS even
θ	1 1 1 1 2 2 3 4 5	NS odd
σ, μ	1 1 1 2 2 3 4 5 6	R even/odd
$\phi + I$	1 1 3 5 10 16 28	NS even
$\phi + \theta$	1 2 4 7 13 21 35	NS odd
$\phi + \sigma, \mu$	1 2 4 8 14 24 40	R even/odd

TABLE I: The edge state counting in the disk geometry. Top table is the number of states of the various sectors of the Ising CFT. Bottom table include the bosonic excitations assuming that the velocities of the bosons and fermions are the same.

charges and such quasiholes when present in an odd number in the bulk do change the physics of the edge modes. This case is called the “twisted” sector^{50–52}. Again these states with F fermion edge modes require $N - F$ to be even. They are properly counted by the fermion field theory above provided we impose now periodic boundary conditions on the field operator $\theta(x + L) = +\theta(x)$. This is the Ramond (R) sector. The boundary conditions imposed on the fermion field operator give rise to different quantization conditions on momenta and hence to different counting of edge modes. In the R (respectively NS) sector, the Majorana fermionic modes are θ_n with n integer (respectively n half-integer).

In the disk without $e/4$ quasiholes in the bulk, for even numbers of electrons we have even numbers of NS Majorana fermions while for odd number of electrons we have odd numbers of NS fermions. This is the case studied by Wen⁴⁹. However, his ED studies in the disk geometry missed the non-Abelian sector associated with the mere existence¹⁹ of fractional charges $e/4$. If we add an extra non-Abelian quasihole for example at the center of disk by tuning an external potential²⁶ we now enter the R sector with again even/odd number of Majorana fermions for even/odd number of electrons. In these studies one has also to consider the elementary charge mode excitations described by the single boson that is already present in simple principal liquids at $\nu = 1/m$. In general the velocities of the edge modes v_n and v_c are not equal. In fact studies in the disk geometry have found estimates of these velocities that are quite different²⁶. They were performed for interactions that are a linear combination of the hard-core three-body interaction Eq.(7) and Coulomb interaction. The mode counting can be performed by elementary means by expanding Bose and Fermi fields into Fourier modes and populating them according to the constraints.

However it is important to realize that the Pfaffian universality class¹⁹ is built upon a 2D CFT which is the product of an Ising model CFT times a free boson with specific radius. This definition as a CFT implies some very specific properties of the spectrum of excited states. Most notably we expect from the existence of the Virasoro algebra of conformal transformation the appearance of so-called conformal towers of states⁵³. In addition to the fermionic Majorana field, the Ising CFT also contains the spin field σ which cannot be expressed locally in terms of the fermion field. As is known from the standard Kramers-Wannier duality of the Ising model, there is also a disorder spin field μ associated to σ by duality. These fields, contrary to the Majorana field, cannot be separated into chirality components. They are boundary-changing operators⁵³ which act upon the boundary conditions of the θ field operator : NS \longleftrightarrow R. In the context of the FQHE the σ, μ operators are associated with the presence of bulk $e/4$ quasiparticles that change the boundary conditions on the edge modes. Finally, as in any CFT there is also the identity operator I .

V. THE PFAFFIAN CONFORMAL TOWERS ON THE CYLINDER

It is known from the representation theory of general CFTs that the spectrum of excited states are arranged into so-called conformal towers of states. In the cylinder geometry with left and right modes, to each primary operator $\Phi_{h, \bar{h}}$ with conformal dimensions (h, \bar{h}) , corresponds an infinite set of states with (dimensionful) energies and momenta :

$$\begin{aligned}
 E &= E_0 + \frac{2\pi v}{L}(h + \bar{h} + n + \bar{n}), \\
 P &= P_0 + \frac{2\pi}{L}(h - \bar{h} + n - \bar{n}),
 \end{aligned}
 \tag{21}$$

where n, \bar{n} are integers, v is the underlying velocity, and E_0, P_0 are respectively the ground-state energy and momentum. There is simply a redefinition by a scale factor $2\pi/L$ with respect to the dimensionless momentum K_{tot} which we use in the remainder of the paper. In the Ising CFT, there are four different sectors created by the action of primary operators on the vacuum. On the cylinder geometry, we need to introduce two Majorana fermions for each edge: θ_L and θ_R . The energy operator ϵ with conformal dimension $h = \bar{h} = 1/2$ of the Ising CFT can be written directly in terms of these fermion fields : $\epsilon = i\theta_L\theta_R$. The four different sectors of the Ising CFT on the cylinder can

$\phi + I + \epsilon$	1 3 11 28 69 152	NS even
$\phi + \theta_{L,R}$	2 6 18 44 104 222	NS odd
$\phi + \sigma, \mu$	1 4 12 32 76 168	R even/odd

TABLE II: The edge state counting in the non-chiral cylinder geometry. This refers to energy level degeneracy taking into account all allowed momenta. We have assumed that Fermi and Bose velocities are equal.

be labeled by their fermionic content. We have the identity with $h = \bar{h} = 0$ and energy tower with $h = \bar{h} = 1/2$, which correspond to NS/even fermion states. Then there is the Majorana sector with $h + \bar{h} = 1/2$ given by NS/odd fermion numbers. These two sectors are created by local Majorana operators $\theta_{L,R}$. Finally, we have the σ and μ sectors with $h = \bar{h} = 1/16$ corresponding to the R sector with respectively even and odd fermionic parity. The information on the counting of states in each sector of the Ising CFT can be extracted from the so-called chiral Virasoro character⁵³:

$$\chi_h(q) = q^{h-c/24} \sum_{n=0}^{\infty} d_h(n) q^n, \quad (22)$$

where c is the central charge, i.e. $c = 1/2$ for the Ising CFT. In the following, we omit the overall $q^{-c/24}$ factor which is needed for modular invariance but not for the counting below. The counting of states in the disk geometry at momentum $\Delta P = 2\pi n/L$ is then given by the integers $d_h(n)$. For the Ising CFT, the different characters are given by⁵³:

$$\begin{aligned} \chi_0(q) &= \frac{1}{2} \left[\prod_{n=0}^{\infty} (1 + q^{n+1/2}) + \prod_{n=0}^{\infty} (1 - q^{n+1/2}) \right] \\ \chi_{1/2}(q) &= \frac{1}{2} \left[\prod_{n=0}^{\infty} (1 + q^{n+1/2}) - \prod_{n=0}^{\infty} (1 - q^{n+1/2}) \right] \\ \chi_{1/16}(q) &= q^{\frac{1}{16}} \prod_{n=1}^{\infty} (1 + q^n). \end{aligned} \quad (23)$$

By expanding the products, we get the counting of states of Table I in each conformal tower of the disk geometry with one edge. By taking into account the Bose field contribution (see Eq. (15)), we deduce the counting of the edge states of the Pfaffian in the disk geometry (see lower table in Table I). In the cylinder geometry, the total number of states in the identity and energy sector is obtained through expansion of $\chi_B^2(\chi_0^2 + \chi_{1/2}^2)$ while the Majorana fermion sector involves $\chi_B^2(2\chi_0\chi_{1/2})$ and the twisted σ sector is related to $\chi_B^2\chi_{1/16}^2$. By expanding the products, we get the counting of states, presented in Table II, in each conformal tower of the Pfaffian at energy $\Delta E = 2\pi v n/L$.

We turn to the ED analysis in the cylinder geometry. The wavefunctions for the edge modes can be written easily through the conformal transformation $z \rightarrow \exp(2i\pi z/L)$. As in the case of the primary Laughlin fluid, we consider the case where there are extra orbitals available in the Fock space beyond those required by the fiducial flux-number of particle relationship. We add a parabolic potential small enough so that there is no mixing between bulk and edge modes. We find the typical low-lying spectrum displayed in Fig.(6). There are clear extremal states that are at the bottom of well-defined towers of excited states. For $K_{tot} = \pm N, \pm 2N, \dots$ these states are global rigid translations of the ground state found at $K_{tot} = 0$. Strictly speaking this statement becomes exact only in the absence of K -space hard walls. Examination of the root configuration of these states reveal their translated nature. They are generated by threading exactly one flux quantum through the cylinder, according to the standard Laughlin gauge argument. However these states do not exhaust the full set of extremal states. There are also arches terminating right in between at $\Delta K_{tot} = \pm N/2$. These states can be generated by transferring a quasiparticle of charge $e/4$ from one side of the cylinder to the other side. This leads to a change of sector in the sense of the previous section. Indeed the operation of quasiparticle transfer is realized by the operator $\sigma e^{i\phi/2}$ in the CFT formulation. The σ field changes the boundary conditions of the fermion field while the vertex operator $e^{i\phi/2}$ takes care of the $e/4$ charge degree of freedom^{19,49}. So we expect that between extremal states with NS-fermion excitations there should be σ sectors with R-fermion excitations. The conformal towers on top of these ground states are different. For even number of particles we have the fully paired Pfaffian and its translated images. They support bosonic excitations and the Ising tower involving the identity operator as well the energy operator⁵⁴. By a shift of $\Delta K_{tot} = N/2$ we find the tower of states associated with the spin field σ and again the boson modes. This scheme is repeated till the droplet is squeezed against the hard wall we impose in the Fock space. For odd number of particles, the alternation is different because the Pfaffian now involves necessarily unpaired fermions. So we have towers generated by the Majorana fermion field with NS boundary

condition. Again by transfer of a $e/4$ quasiparticle we switch to the spin μ sector which has the same structure as the σ sector in the N even case. Our findings are in perfect agreement with the CFT scheme for the low-lying states provided the Bose and Fermi velocities are equal. The identification of states becomes obvious in the TT limit as can be seen in Fig.(7). Here we plot the three distinct conformal towers on a wide cylinder in the left panel and in the TT limit in the right panel. The CFT degeneracies are marked close to each multiplet of states. The counting is in perfect agreement with the CFT numbers obtained from Table (II). In this TT limit it is easy to check that the Fermi and Bose velocities are indeed equal. This raises the question whether this apparent equality on wide cylinders is a correct feature of the thermodynamic limit or if it is simply a remnant of the TT limit. The ED data alone are not enough to answer convincingly this question because the wide cylinders quickly require too many particles. We thus turn to another type of method using the knowledge of wavefunctions which does not have this limitation.

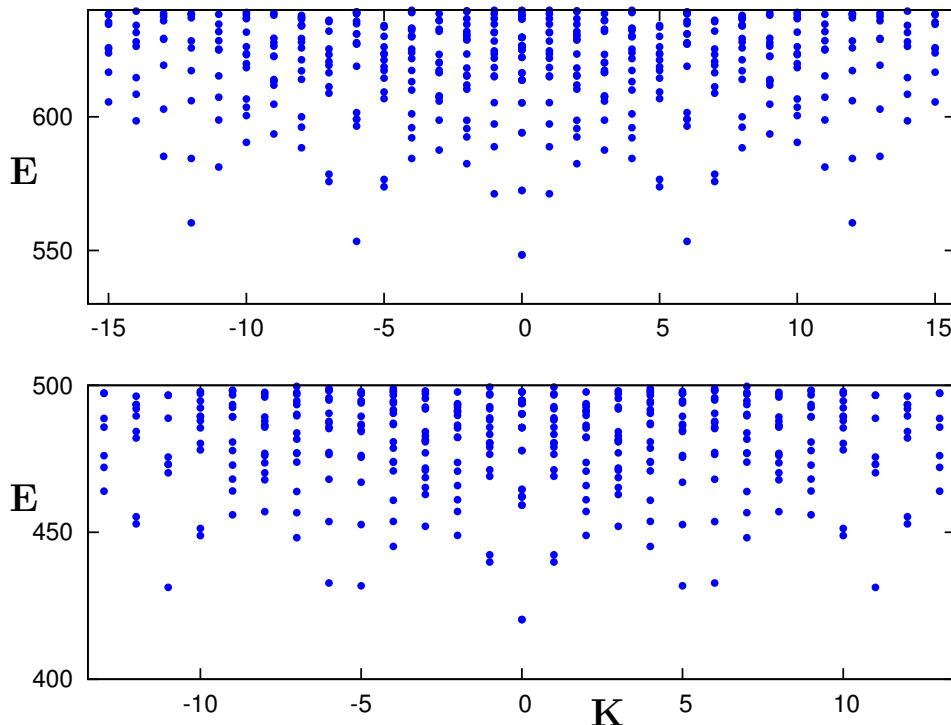


FIG. 6: Top panel : the edge excitation sector for an even number of electrons $N_e = 12$. The absolute ground state is at $K = 0$ and generates the identity plus energy tower of the Ising sector in addition to the charge excitations. This structure of states repeats itself for $K = \pm N_e, \pm 2N_e, \dots$. This explains only half of the towers. For $K = \pm N_e/2, \pm 3N_e/2, \dots$ we assign the tower structure to the σ tower of states with the extra charge modes. This is consistent provided the velocities v_n and v_c are almost equal. Bottom panel : the odd number case with $N_e = 11$. Now the absolute ground state is the twisted Pfaffian state Eq.(33) and it supports the μ tower of states which is identical to the σ tower. Next to it, we observe the Majorana tower of states with characteristic (quasi) doubly degenerate ground states. Energies are in units of β .

VI. MEASURING SCALING DIMENSIONS BY A MONTE-CARLO METHOD

While the conformal tower structure is readily apparent in ED studies even for a modest number of particles, it is not easy to derive scaling dimensions within the confines of this method. In fact we find that only the global charge Luttinger parameter can be evaluated reliably. The knowledge of the Pfaffian CFT Ising \times U(1) predict also the scaling dimensions of all conformal towers including notably the non-Abelian σ tower with scaling dimension $1/8$. We first note that treating the potential term in first-order perturbation theory is in fact enough to describe the emergence of conformal towers by giving nonzero velocities to all low-energy modes. So another strategy is to use the exact knowledge of wavefunctions in the absence of the perturbing potential and to evaluate energies by taking the expectation value of the potential with respect to these unperturbed states : this is first-order perturbation theory with respect to the parabolic potential. The full description of edge states given in section V is adequate for this purpose.

We first consider the case of an even number of particles with the center of mass of the Pfaffian wavefunction

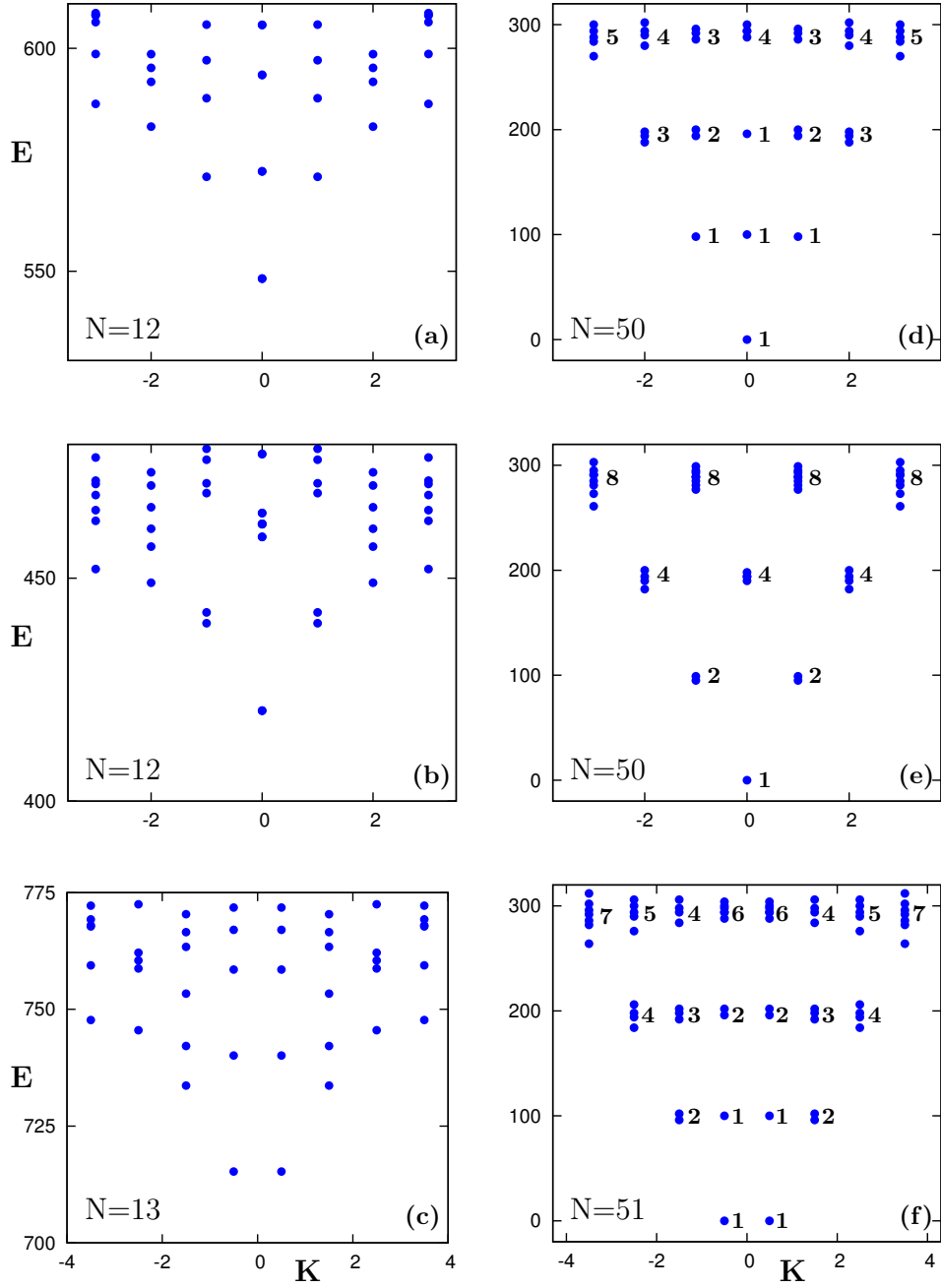


FIG. 7: Identification of CFT towers of states in the FQH regime where the cylinder is large enough (left-hand side) and in the TT limit (right-hand side). The identity+energy tower is displayed in (a) and (d). The σ tower is in (b) and (e). Finally the Majorana tower is given in (c) and (f). When the cylinder radius is sent to small values, the TT limit, the conformal towers become obvious. In the TT limit the numbers are the degeneracies obtained in Table II. Energies are in units of β .

coinciding with the minimum of the parabolic confining potential. The spectrum of edge modes for $N = 12$ in such a configuration is shown in the top panel of Fig.(6). If we note $E_n(K)$ the n th lowest energy at momentum K , one can estimate the velocities v_c and v_n inside the identity+energy CFT tower on top of the Pfaffian state by the following differences :

$$E_1(1) - E_1(0) = \frac{2\pi}{L} v_c, \quad (24)$$

$$E_2(0) - E_1(0) = \frac{2\pi}{L} v_n, \quad (25)$$

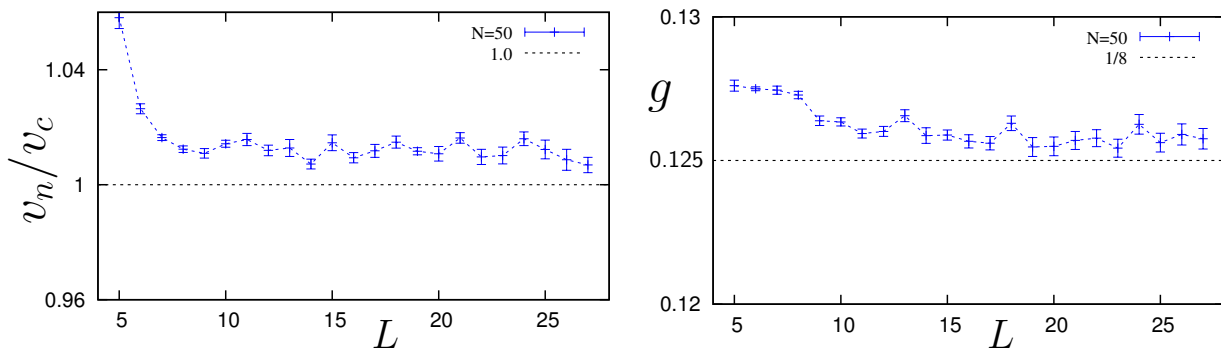


FIG. 8: Left panel : The ratio of the Bose and Fermi velocities measured by the Monte-Carlo procedure as a function of the perimeter of the cylinder L for $N=50$ particles. The evidence is for the equality of the two velocities in the thermodynamic limit as required by the interpretation of the conformal towers. We indicate confidence intervals with a width equal to twice the standard deviation. Right panel : measurements of the Luttinger parameter of the bosonic part of edge modes using the same method. Results are in agreement up to a few percent with the theoretical value $g = 1/8$ at the thermodynamic limit ($N \rightarrow +\infty$ and $L \rightarrow \infty$).

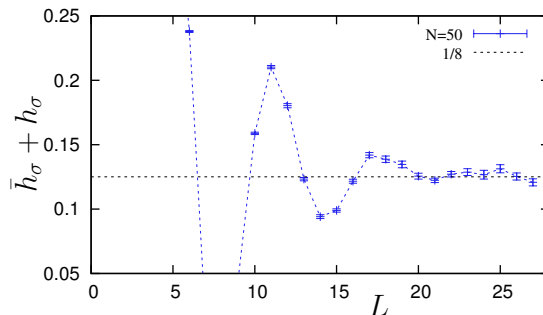


FIG. 9: The scaling dimension of the σ spin field computed by the energy of lowest-lying state of the corresponding conformal tower. It converges towards the expected value $1/8$. Note that we need large values of L to obtain convergence (for $N=50$).

at leading order in the number of particles. Every conformal tower for fixed number of particles can be indexed by the current quantum number $J = n_R - n_L$ (even) which counts the transfer of fractional charges $en_{L,R}/4$ between edges, hence $J = 0, \pm 2, \pm 4, \dots$. Ground states of those towers have momenta $K = JN/4$, and their relative energies are given by the Luttinger parameter g which characterizes the energy needed to transfer a charge $e/4$ from one side to the other of the droplet, and the scaling dimension of the spin primary field, $\bar{h}_\sigma + h_\sigma = 1/8$, which gives the cost in energy to change the boundary conditions of the θ field. More precisely, if we look at successive conformal towers indexed by the current quantum number J , the ground state energies of each tower are, according to the effective theory explained in the previous section :

$$E_1\left(\frac{1}{4}JN\right) - E_1(0) = \frac{\pi}{2L}v_c g J^2 + \delta_{J/2, \text{odd}} \frac{2\pi}{L}v_n(\bar{h}_\sigma + h_\sigma), \quad (26)$$

where $\delta_{J/2, \text{odd}}$ is unity if $J/2$ is odd, zero otherwise. In particular, we deduce the g parameter from Eqs(8,9) and the estimation of v_c through:

$$E_1(N) - E_1(0) = \beta N = \frac{2\pi}{L}v_c g. \quad (27)$$

We can use exact diagonalizations up to $N \leq 14$ to measure velocities v_c and v_n from Eqs.(24,25). For better precision for this small number of particles, we also take into account the next-to-leading order in variation with N in Eqs.(24,25). At fixed L and fixed value of the confining potential β , the velocities v_c and v_n scale as N because the slope of the parabolic confining potential at the position of the edge grows like N at leading order. We assume the simple scaling: $v = \alpha N + \gamma + O(1/N)$ which is true in the TT limit. To measure the leading term, we first check that N is large enough such that $v_{c,n}(N)$ are linear, and then take the slope obtained with the last two points from the largest values of N .

We observe that $v_c \approx v_n$ for $L \lesssim 15$, i.e. when the two counterpropagating edge are far enough and there is no interaction between them. From the v_c measurement, we are also able to compute the Luttinger parameter g . We obtain $g \approx 1/8$ as expected in the whole range $0 \leq L \lesssim 15$. However the practical limit $N \leq 14$ does not allow to measure the conformal dimensions $\bar{h}_\sigma + h_\sigma$ and $\bar{h}_\theta + h_\theta$.

To circumvent the size limit, we use the Metropolis Monte Carlo algorithm to compute energies of eigenstates for which we have an exact first quantized expression. Indeed, as long as the external potential is infinitesimal, we know the explicit expressions of some of the low-lying states. As previously mentioned, the highest-density state which lives at the bottom of the identity+energy tower is the cylinder Moore-Read Pfaffian wavefunction deduced from Ψ_{MR} of Eq.(17). Then, $E_1(0) = \langle \Psi_{MR} | \sum_i V(x_i) | \Psi_{MR} \rangle$, which can be computed directly in real space through a $2N$ -dimensional integration. For $N = 50$ and $O(10^9)$ Monte-Carlo steps, we obtain a relative precision of 10^{-5} over the energy. Other energies can be obtained in the same way. The energy $E_1(1)$ is the mean energy of a bosonic excitation of momentum $K_{tot} = +1$ localized at the right edge of the Moore-Read state :

$$b_1^{R\dagger} \Psi_{MR}(Z_i) \propto \left\{ \sum_i Z_i \right\} \Psi_{MR}(Z_i). \quad (28)$$

The state which corresponds to one pair of Majorana fermion excitations of momentum $\pm 1/2$ at each edge of the droplet can be written as :

$$\Psi_{-1/2,+1/2} = \mathcal{A} \left(Z_1^{-1} Z_2^0 \frac{1}{Z_3 - Z_4} \cdots \frac{1}{Z_{N-1} - Z_N} \right) \prod_{i < j} (Z_i - Z_j)^m, \quad (29)$$

and its mean energy is $E_2(0)$. At the bottom of the σ tower we have the twisted Pfaffian wavefunction :

$$\Psi^{Twisted} = \text{Pf} \left(\frac{Z_i + Z_j}{Z_i - Z_j} \right) \prod_{i < j} (Z_i - Z_j)^m, \quad (30)$$

whose mean energy is $E_1(N/2)$. From the four energies, $E_1(0), E_1(1), E_2(0)$ and $E_1(N/2)$, we can deduce by Eqs.(24,25,26,27) estimates of the velocities v_c, v_n , the charge Luttinger parameter g , and the scaling dimension $\bar{h}_\sigma + h_\sigma$.

Our results for 50 particles and $0 < L \lesssim 30$ are shown in Figs.(8,9). Each energy is computed with 5×10^9 MC steps. To estimate the standard deviation of each point we use the binning method. Indeed, we separate the process into M successive bins, average energies onto each bin, obtain M independent estimations of the quantity to compute, and estimate the standard deviation from the M binned values. We choose a bin size of a few 10^8 steps so that our M estimations are statistically independent. We find that $v_c \approx v_n$ up to 2 – 3 percent for $0 < L \lesssim 25$. The imprecision comes both from the MC fluctuations and the next-to-leading order in variation with N in Eqs.(24,25). This strongly suggests that the two velocities are equal at the thermodynamic limit. Similarly, we observe for $0 < L \lesssim 25$ that the Luttinger parameter $g \approx 1/8$ as expected up to a few percent. Estimations of $\bar{h}_\sigma + h_\sigma$ are in agreement with the expected $1/8$ for large enough value of L . The correct Ising CFT exponent that we obtain for the non-Abelian sector built upon the σ field is an important check of the CFT construction.

To measure the conformal dimension $\bar{h}_\theta + h_\theta$ of the Majorana field operator, we compute the energies of states in the N odd sector. For N odd, there is an odd number of Majorana fermions in the untwisted sector. We then use the three wavefunctions :

$$\Psi_{+1/2} = \mathcal{A} \left(Z_1^0 \frac{1}{Z_2 - Z_3} \cdots \frac{1}{Z_{N-1} - Z_N} \right) \prod_{i < j} (Z_i - Z_j)^m \quad (31)$$

$$b_1^{R\dagger} \Psi_{+1/2} = \left\{ \sum_i Z_i \right\} \Psi_{+1/2} \quad (32)$$

$$\Psi^{odd, Twisted} = \mathcal{A} \left(Z_1^0 \frac{Z_2 + Z_3}{Z_2 - Z_3} \cdots \frac{Z_{N-1} + Z_N}{Z_{N-1} - Z_N} \right) \prod_{i < j} (Z_i - Z_j)^m \quad (33)$$

and compute their energies in order to get an estimate of $\bar{h}_\theta + h_\theta$. We find that $\bar{h}_\theta + h_\theta = 0.50(3)$ for $L = 25, N = 50$, which is in agreement with the CFT expectation $1/2$.

VII. CONCLUSION

We have studied the edge modes of the filling fractions $\nu = 1/3$ and $\nu = 5/2$ in the QPC geometry by using model wavefunctions of Laughlin and Moore-Read type. These functions are generated numerically by using ED of special

hard-core Hamiltonians. They are believed to capture the physics of the more realistic Coulomb potential for 2DEGs. In the case of the $\nu = 1/3$ QPC we have shown that this geometry is suited to explore the electron-quasiparticle duality. It allows measurement of the Luttinger parameter in the case of electron tunneling in a simple way.

In the Moore-Read Pfaffian case, we have studied in detail the conformal tower of states that are expected from the 2D CFT foundations of this universality class of incompressible quantum fluids. The cylinder geometry allows us to study the non-Abelian σ sector in a simple way : the corresponding CFT tower is found by choosing the appropriate total momentum. There is no need to impose by hand the presence of a $e/4$ quasiparticle as is the case in the sphere or disk geometry. The CFT towers becomes very clear in the TT limit. Extracting the correct scaling dimensions requires however to choose a regime with reasonably large circumference L and enough electrons. While ED is enough to get the global charge Luttinger exponent, this does not allow the determination of the other scaling dimensions. For this purpose, we have introduced a simple Monte-Carlo method based on the exact formulas for edge modes given in Ref.(50). This Metropolis evaluation of energies in a perturbing potential leads to estimates of the scaling of the spin field σ as well as the Majorana field θ that are in agreement with the Ising CFT values. We emphasize that this strategy is applicable to models whose relevant wavefunctions are given by an analytical formula for which an efficient metropolis update is feasible. While previous works^{55,56} have given evidence for the correct CFT counting of non-Abelian quasiholes, we have in this paper uncovered the complete Virasoro structure of the CFT towers. The equality of Bose and Fermi velocities of the edge modes also implies as noted in Ref.(50) that the special theory defined by the three-body hard-core model Eq.(7) has a hidden superconformal $N=2$ symmetry at level $k=2$. We have found that a similar symmetry enhancement happens also for the bosonic Pfaffian at $\nu = 1$ which has Kac-Moody symmetry $SU(2)$ at level $k=2$.

Finally we stress that the potential added along the cylinder is by no means limited to the simple parabolic shape we have explored. It may be modified to explore more complex, experimentally relevant configurations. Recent work^{57,58} have also explored the cylinder geometry with the entanglement spectrum point of view and offer a complementary view of the 2D CFT-based FQH wavefunctions.

Acknowledgments

We acknowledge discussions with P. Roche.

-
- ¹ S. Datta, "Electronic transport in mesoscopic systems", Cambridge University Press, Cambridge UK, 1995.
 - ² L. Saminadayar, D. C. Glattli, Y. Jin, and B. Etienne, Phys. Rev. Lett. **79**, 2526 (1997).
 - ³ R. de Picciotto, M. Reznikov, M. Heiblum, V. Umansky, G. Bunin, and D. Mahalu, Nature **389**, 162 (1997).
 - ⁴ R. B. Laughlin, Phys. Rev. Lett. **50**, 1395 (1983).
 - ⁵ A. H. MacDonald, Phys. Rev. Lett. **64**, 220 (1990).
 - ⁶ X. G. Wen, Phys. Rev. **B41**, 12838 (1990).
 - ⁷ X. G. Wen, Int. J. Mod. Phys. **B6**, 1711 (1992).
 - ⁸ X. G. Wen, Adv. Phys. **44**, 405 (1995).
 - ⁹ S. Jolad, C. C. Chang, and J. K. Jain, Phys. Rev. **B75**, 165306 (2007).
 - ¹⁰ S. Jolad, D. Sen, and J. K. Jain, Phys. Rev. **B82**, 075315 (2010).
 - ¹¹ S. Jolad and J. K. Jain, Phys. Rev. Lett. **102**, 116801 (2009).
 - ¹² G. J. Sreejith, S. Jolad, D. Sen, and J. K. Jain, Phys. Rev. **B84**, 245104 (2011).
 - ¹³ A. M. Chang, Rev. Mod. Phys. **75**, 1449 (2003).
 - ¹⁴ V. J. Goldman and E. V. Tsiper, Phys. Rev. Lett. **86**, 5841 (2001); E. V. Tsiper and V. J. Goldman, Phys. Rev. **B64**, 165311 (2001).
 - ¹⁵ X. Wan, F. Evers, and E. H. Rezayi, Phys. Rev. Lett. **94**, 166804 (2005).
 - ¹⁶ J. J. Palacios and A. H. MacDonald, Phys. Rev. Lett. **76**, 118 (1996).
 - ¹⁷ E. Papa and A. H. MacDonald, Phys. Rev. Lett. **93**, 126801 (2004).
 - ¹⁸ U. Zülicke, J. J. Palacios, and A. H. MacDonald, Phys. Rev. **B67**, 045303 (2003).
 - ¹⁹ G. Moore and N. Read, Nucl. Phys. **B360**, 362 (1991).
 - ²⁰ C. Nayak, S. H. Simon, A. Stern, M. Freedman, and S. Das Sarma, Rev. Mod. Phys. **80**, 1083 (2008).
 - ²¹ Xin Wan, Kun Yang, and E. H. Rezayi, Phys. Rev. Lett. **97**, 256804 (2006).
 - ²² Hua Chen, Zi-Xiang Hu, Kun Yang, E. H. Rezayi, and Xin Wan, Phys. Rev. **B80**, 235305 (2009).
 - ²³ Xin Wan, Zi-Xiang Hu, E. H. Rezayi, and Kun Yang, Phys. Rev. **B77**, 165316 (2008).
 - ²⁴ Hua Chen, Zi-Xiang Hu, Kun Yang, E. H. Rezayi, and Xin Wan, Phys. Rev. **B80**, 235305 (2009).
 - ²⁵ Zi-Xiang Hu, E. H. Rezayi, Xin Wan, and Kun Yang, Phys. Rev. **B80**, 235330 (2009).
 - ²⁶ Zi-Xiang Hu, Ki Hoon Lee, E. H. Rezayi, Xin Wan, Kun Yang, New J. Phys. **13**, 035020 (2011).
 - ²⁷ C. de C. Chamon and X. G. Wen, Phys. Rev. **B49**, 8227 (1994).

- ²⁸ P. Soulé and Th. Jolicoeur, Phys. Rev. **B85**, 155116 (2012).
- ²⁹ Z.-X. Hua, Z. Papic, S. Johri, R. N. Bhatt, and P. Schmitteckert, Phys. Lett. A **376**, 2157 (2012).
- ³⁰ F. D. M. Haldane, J. Phys. C **14**, 2585 (1981).
- ³¹ C. L. Kane and M. P. A. Fisher, Phys. Rev. **B46**, 15 233 (1992).
- ³² C. L. Kane and M. P. A. Fisher, Phys. Rev. Lett. **68**, 1220 (1992).
- ³³ C. L. Kane and M. P. A. Fisher, Phys. Rev. Lett. **72**, 724 (1994).
- ³⁴ C. L. Kane and M. P. A. Fisher, Phys. Rev. **B51**, 13 449 (1995).
- ³⁵ C. L. Kane, M. P. A. Fisher, and J. Polchinski, Phys. Rev. Lett. **72**, 4129 (1994).
- ³⁶ R. Tao and D. J. Thouless, Phys. Rev. **B28**, 1142 (1983).
- ³⁷ D. J. Thouless, Surf. Sci. **142**, 147 (1984).
- ³⁸ S. T. Chui, Phys. Rev. Lett. **56**, 2395 (1986).
- ³⁹ E. J. Bergholtz, T. H. Hansson, M. Hermanns, and A. Karlhede, Phys. Rev. Lett. **99**, 256803 (2007).
- ⁴⁰ E. J. Bergholtz and A. Karlhede, Phys. Rev. Lett. **94**, 026802 (2005); J. Stat. Mech. (2006) L04001; Phys. Rev. B **77** 155308 (2008).
- ⁴¹ A. Seidel, H. Fu, D.-H. Lee, J. M. Leinaas, and J. Moore, Phys. Rev. Lett. **95**, 266405 (2005).
- ⁴² E. Ardonne, Phys. Rev. Lett. **102**, 180401 (2009).
- ⁴³ E. H. Rezayi and F. D. M. Haldane, Phys. Rev. **B50**, 17199 (1994).
- ⁴⁴ R. Thomale, A. Sterdyniak, N. Regnault, and B. A. Bernevig, Phys. Rev. Lett. **104**, 180502 (2010).
- ⁴⁵ A. Sterdyniak, A. Chandran, N. Regnault, B. A. Bernevig, and P. Bonderson, Phys. Rev. **B85**, 125308 (2012).
- ⁴⁶ A. M. Läuchli, E. J. Bergholtz, J. Suorsa, and M. Haque, Phys. Rev. Lett. **104**, 156404 (2010).
- ⁴⁷ N. Regnault and Th. Jolicoeur, Phys. Rev. Lett. **91**, 030402 (2003); Phys. Rev. **B69**, 235309 (2004).
- ⁴⁸ C.-C. Chang, N. Regnault, Th. Jolicoeur, and J. K. Jain, Phys. Rev. **A72**, 013611 (2005).
- ⁴⁹ X. G. Wen, Phys. Rev. Lett. **70**, 355 (1993).
- ⁵⁰ M. Milovanovic and N. Read, Phys. Rev. **B53**, 13559 (1996).
- ⁵¹ P. Fendley, M. P. A. Fisher, and C. Nayak, Phys. Rev. Lett. **97**, 036801 (2006).
- ⁵² P. Fendley, M. P. A. Fisher, and C. Nayak, Phys. Rev. **B75**, 045317 (2007).
- ⁵³ P. Ginsparg, “Applied Conformal Field Theory”, Les Houches lectures, published in “Fields, Strings, and Critical Phenomena”, ed. by E. Brezin and J. Zinn-Justin, North-Holland (1989).
- ⁵⁴ Malte Henkel, “Conformal Invariance and Critical Phenomena”, Springer Verlag, Berlin (1999).
- ⁵⁵ N. Regnault and Th. Jolicoeur, Phys. Rev. **B76**, 235324 (2007).
- ⁵⁶ N. Read and E. H. Rezayi, Phys. Rev. **B59**, 8084 (1999).
- ⁵⁷ M. P. Zaletel, R. S. K. Mong, and F. Pollmann, Phys. Rev. Lett. **110**, 236801 (2013).
- ⁵⁸ D. Varjas, M. P. Zaletel, and J. E. Moore, eprint arXiv:1306.4976